

CHAPTER «PHYSICAL AND MATHEMATICAL SCIENCES»

NANOSTRUCTURED COATINGS ZrN, OBTAINED BY VACUUM-ARC DEPOSITION METHOD

Nataliia Pinchuk¹

Oleksandr Terletskyi²

DOI: <https://doi.org/10.30525/978-9934-26-221-0-1>

Abstract. Nowadays increased interest is shown in ZrN coatings, which have high erosion resistance, strength in combination with a fairly high hardness. Among the various ion-plasma techniques, vacuum-arc is one of the most versatile processes due to the high degree of ionization of the flow of film-forming particles and good adhesion properties of coatings to the substrate. *The purpose* of the paper is problem of structural engineering of vacuum-arc ZrN coatings is acute in order to predictably obtain the necessary functional physical and mechanical characteristics. *Methodology.* The study of the structure and phase composition of research samples of ZrN coatings was carried out by methods of optical, electron microscopy, X-ray diffraction analysis. The elemental composition was determined using the X-ray fluorescence method and energy-dispersive X-ray spectroscopy (EDS). Mechanical tests of materials were performed in the mode of microindentation, in particular – active loading, using the Berkovich pyramid (installation according to ISO 14577). *Results.* It is established that the formation of the bitexture state with the axes [111] + [311] occurs under the action of the impulse bias potential (U_i) -800 V, even at the lowest constant bias potential (U_c) -27 V. In ZrN coatings at high values of $U_c = -200$ V, in the whole range of pulse potentials, is the formation of

¹ Candidate of Physical and Mathematical Sciences,
Researcher, Department of Materials Science,
National Technical University «Kharkiv Polytechnic Institute», Ukraine

² Candidate of Physical and Mathematical Sciences,
Associate Professor, Department of Materials Science,
National Technical University «Kharkiv Polytechnic Institute», Ukraine

the texture with the axis [111]. The change in substructural characteristics is nonmonotonic. Growth is observed. A generalized diagram of the axial texture axis is constructed, with the help of which it is possible to choose those deposition conditions that will provide coatings with a given set of properties. Proposed the integral parameter $PU = pN (U_c + \tau \cdot f \cdot U_i)$ for the analysis of the obtained data. *Practical implications.* Based on the proposed physical concepts, the conditions for obtaining ion-plasma vacuum-arc coatings ZrN, which affect the structure, substructure and mechanical properties, have been developed. *Value/originality.* Physical mechanisms in the formation of the ZrN phase, when radiation damage occurs and at the same time the process of relaxation of structural defects, which are realized under the action of heat fluxes. Depending on the intensity and duty cycle of high-energy impact, the corresponding axial textures, internal stresses, and, as a consequence, a change in functional properties are formed.

1. Introduction

In recent years, transition metal nitrides are widely used as protective coatings for industrial applications [1–3]. Obtained in the presence of a chemically active nitrogen atmosphere, the precipitated nitride coatings provide a wide variation in the microstructure of the material by changing the grain size, crystallo-graphic orientation, lattice defects, texture, and surface microstructure and phase composition. Unfortunately, the physical and mechanical characteristics of the coatings obtained in this case differ significantly (sometimes by orders of magnitude) depending on the deposition technology and specific parameters of the growth process.

Therefore, an important task today is to establish the general patterns of formation of coatings from the main technological parameters. The aim of the work is to study the influence of working pressure, constant bias potential and high-energy pulse stimulation on the phase composition, structure and hardness of vacuum-plasma ZrN coatings. Increased interest is shown in ZrN coatings, due to their high erosion resistance, strength combined with a fairly high hardness. Also, such interest is associated with the intensive development of radiation technologies and the use of ZrN coatings as a radiation-resistant material.

In this regard, the scientific and practical task of structural engineering of vacuum-arc ZrN coatings is urgent in order to predictably obtain the

necessary structural states and functional physical and mechanical characteristics.

2. Methods of obtaining and research coatings

Substantiates the choice of production technology and methods of studying the structure and properties. Vacuum-arc coatings with a thickness of 9-13 μm , obtained on the modernized Bulat-6 installation, namely ZrN coatings, which were deposited on Stainless steel plates 12Cr18Ni10Ti (analog of stainless steel SS 321), were studied. Technological conditions of deposition: nitrogen atmosphere pressure (meaning N_2) $p\text{N} = (0.133\dots 0.63)$ Pa; constant potential (U_c) -27 V, -150 V and -220 V, pulse potential (U_i) -800 V, -1200 V, -2000 V with a du-ratio of $\tau = 7$ μs and a ripple frequency of 7 kHz, i.e., with an interval between them of 143 μs .

Structural studies of the samples were performed on the installation “DRON-3M”. Cu-K α radiation was used in all studies. The analysis of substructural characteristics was performed by the method of approximation of the form of diffraction reflexes for two orders of magnitude from the planes of the crystal lattice using the Cauchy approximation function. To study the stress-strain state, the method of multiple oblique surveys (“a-sin² ψ ”-method) and the method of crystal groups were used. Micro- and nanoindentation on hardness was performed at the Micron-gamma installation with a Berkovich diamond pyramid.

3. Morphology of ZrN coatings

The influence of the constant potential on the morphology of ZrN coatings was analyzed. Thus, coatings obtained at a relatively low constant bias potential of -40 V, have a large enough amount of drip phase, both in volume and on the surface (Figure 1 a, b). It does not have a pronounced columnar structure. Figure 1 c, d shows the morphology of the surface and the fractogram of the fracture of the coatings obtained by applying the bias potential of the value of $U_c = -220$ V. It is seen that the coatings are virtually no microparticles of the drip phase, both in volume and on the surface the growth of the coating has a columnar appearance (Figure 1 c). This significant decrease in the droplet phase content can be explained by the fact that the droplet component in the plasma acquires a negative

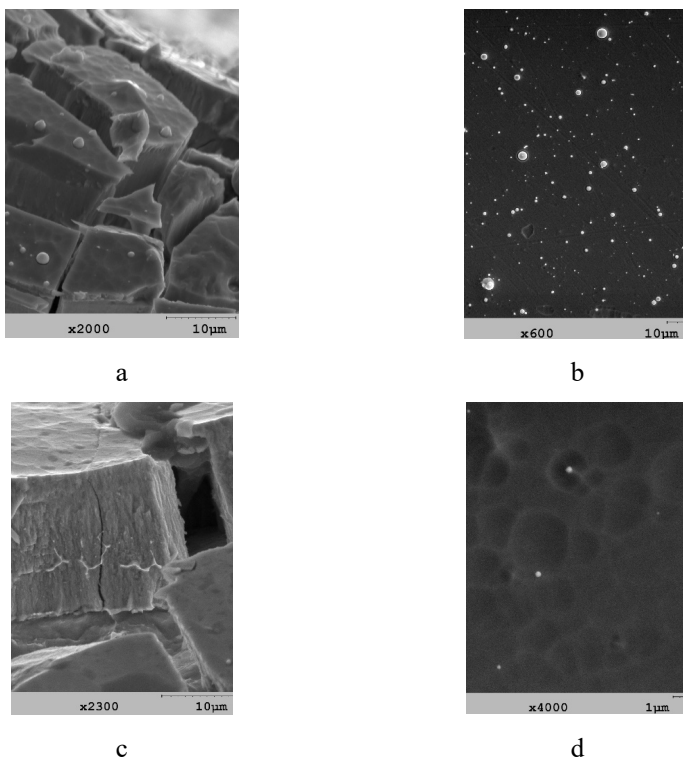


Figure 1. Fractograms of fractures and surface morphology of ZrN coatings ($pN = 0.65$ Pa): a, b – $U_c = -40$ V; c, d – $U_c = -220$ V

(“floating”) potential and is repelled by the surface to which the negative potential is applied (in this case the substrate surface) [4].

4. X-ray phase analysis of ZrN coatings

Three series of vacuum-arc ZrN coatings were obtained with the following deposition conditions: 1) influence of only constant potential (-27 V, -150 V and -220 V) without additional pulse stimulation; 2) at low constant potential ($U_c = -27$ V....-30 V) the influence of the pulse potential on the peculiarities of ZrN formation of coatings was determined; 3) simultaneous supply of large constant (-150... -220) V and pulse potentials.

Figure 2 shows the diffraction spectra of ZrN coatings obtained by the first deposition scheme. It is seen that for all values of the constant bias potential (-27 ... -300) V, a single-phase structural state characteristic of ZrN with a face-centered cubic lattice (structural type NaCl) is formed (ICDD PDF-2 № 35-0753).

In this case, depending on the magnitude of the negative shear potential, the ratio of the intensities of the diffraction peaks from different planes changes, which indicates the appearance of texture (predominant orientation of the crystallites). At low bias potential (-27 ... -40) V the high intensity of the peak from the plane (200) indicates textures with the axis [100] (Figure 2, spectrum 2), which is perpendicular to the plane of growth. With increasing U_c , the texture changes: at $U_c = -150$ V – to the bitexture state with the predominant orientation of crystal-lites with axes [111] and [311] perpendicular to the growth plane, and at $U_c = -220$ V changes to almost uniaxial texture with the axis [111] (see Figure 2, spectrum 4).

According to the second deposition scheme, ZrN coatings were obtained at the lowest value of the constant potential ($U_c = -27$ V), but under the action of high-potential potential in pulsed form with a duration of 7 μ s.

When the potential $U_i = -800$ V is applied, there is a noticeable increase in the intensity of the peak (311) and the formation of the bitexture state with the axes [111] and [311] (Figure 3, spectrum 1). It should be noted that at $U_i = -1200$ V ($U_c = -27$ V) there is no texture [100]. In this case, the supply of U_i at a small value of U_c stimulates the formation of the texture with the axis [110], which is manifested in the increased reflection from the plane (220) (Figure 3, spectra 2).

The supply of the greatest potential $U_i = -2000$ V leads to the strengthening of the texture with the axis [110] at the lowest $U_c = -27$ V with a decrease in the region of the bitextural state [311] and [111] (Figure 3, spectrum 3).

Next, the influence of high-voltage pulse potential with amplitudes of -800 V, -1200 V and -2000 V (third deposition scheme) was analyzed, the results are presented in Figures 4 and 5, precipitated at different pressures of nitrogen atmosphere.

It is seen that the tendency of transition from the bitextural state (with the texture axes [311] and [111]) at $p_N = (0.1... 0.3)$ Pa to monotextural (with the texture axis [111]) at $p_N > 0.3$ Pa (Figure 5) by analogy with

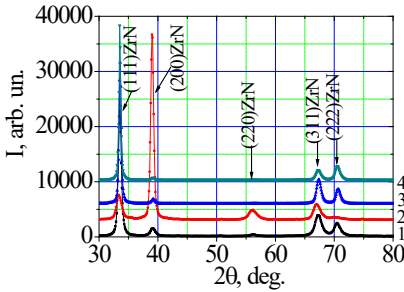


Figure 2. X-ray diffraction spectra from ZrN coatings obtained without ad-ditional pulse stimulation at:

- 1 – $U_c = -150$ V, $pN = 0.133$ Pa;
- 2 – $U_c = -30$ V, $pN = 0.63$ Pa;
- 3 – $U_c = -150$ V, $pN = 0.63$ Pa;
- 4 – $U_c = -220$ V, $pN = 0.63$ Pa

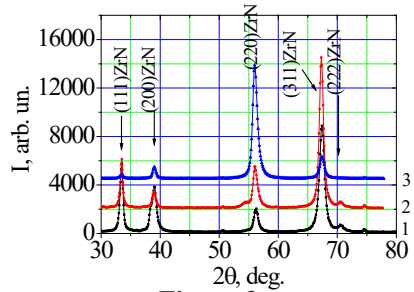


Figure 3.

X-ray diffraction spectra from ZrN coatings obtained at ($\tau = 7 \mu s, pN = 0.63$ Pa):

- 1 – $U_c = -(5... .8)$ V, $U_i = -800$ V;
- 2 – $U_c = -27$ V, $U_i = -1200$ V;
- 3 – $U_c = -27$ V, $U_i = -2000$ V

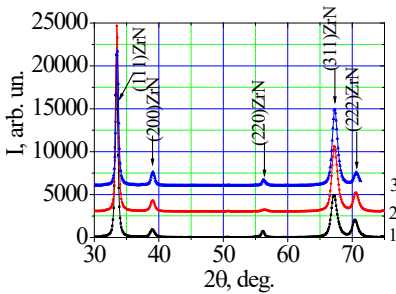


Figure 4. X-ray diffraction spectra from ZrN coatings obtained at ($\tau = 7 \mu s, U_c = -150$ V):

- 1 – $U_i = -800$ V, $pN = 0.16$ Pa;
- 2 – $U_i = -1200$ V, $pN = 0.133$ Pa;
- 3 – $U_i = -2000$ V, $pN = 0.133$ Pa

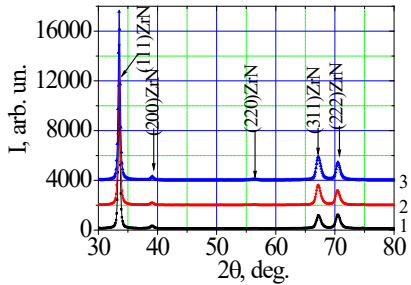


Figure 5. X-ray diffraction spectra from ZrN coatings obtained ($\tau = 7 \mu s, U_c = -150$ V):

- 1 – $U_i = -800$ V, $pN = 0.4$ Pa;
- 2 – $U_i = -1200$ V, $pN = 0.63$ Pa;
- 3 – $U_i = -2000$ V, $pN = 0.63$ Pa

the modes of application without pulse stimulation) is preserved in this case. The action for 7 % of the time with an amplitude of the bias potential of -800 V at a relatively low pressure of $p_N < 0.1$ Pa lead to the appearance of a bitexture state with the axes [110] and [311]. As the value of the negative impulse potential applied to the substrate increases to -2000 V, the degree of perfection of this bitextural state increases (Figure 4, spectrum 3).

The supply of $U_c = -220$ V with the simultaneous action of pulse potentials leads to the formation of almost uniaxial texture with the axis [111] (Figure 6). However, in contrast to the formation of the coating without pulse stimulation, the supply of $U_i = -2000$ V lead to a slight decrease in the relative intensity (111) (ie, a decrease in the degree of texturing with the axis [111]) (see Figure 6, spectrum 2).

Thus, the supply of U_i leads to a significant change in the predominant growth of crystallites at low values of U_c , as well as their degree of perfection.

5. The texture parameter (Phkl) of ZrN coatings

Harris' method was used to determine the texture parameter [5–7]. The texture parameter P_{hkl} for the main planes in the coatings obtained for the three modes was determined. Figures 7-9 show the corresponding dependences for the 4 main reflection planes (111), (200), (220) and (311).

It is seen that at a relatively low constant bias potential (up to -50 V) without impulse influence (first series) is the formation of the texture with the axis [100] (Figure 7 b). Increasing the potential to -100 V leads to a new type of texture with the axis [311] (Figure 7 d). At higher potentials, when the determining factor is the deformation factor – the formation of texture [111] (Figure 7 a).

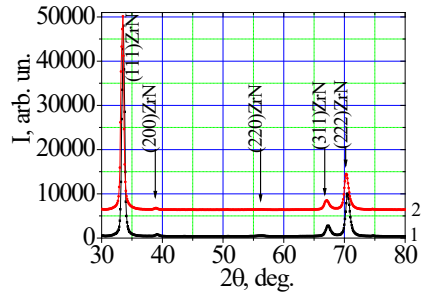


Figure 6. X-ray diffraction spectra from ZrN coatings obtained ($\tau = 7 \mu s, U_c = -220$ V):
1 – $U_i = -1200$ V, $p_N = 0.63$ Pa;
2 – $U_i = -2000$ V, $p_N = 0.63$ Pa

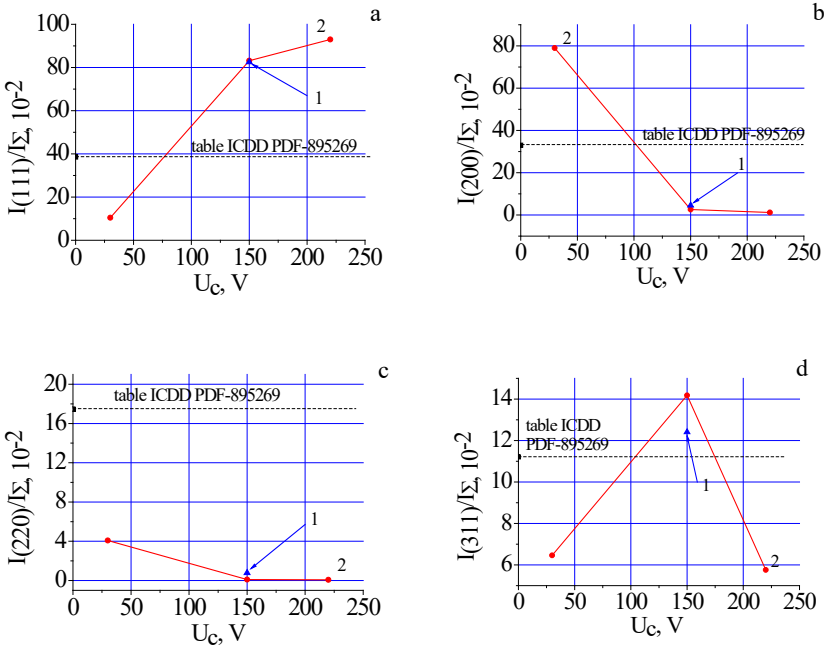


Figure 7. Dependence of the texture parameter P_{hkl} for the first series of ZrN coatings on the value of U_c for different planes: a – (111), b – (200), c – (220), d – (311); 1 – $p_N = 0.133$ Pa, 2 – $p_N = 0.63$ Pa

The presence of high-voltage pulse potential qualitatively changes the nature of texture formation at low constant bias potential (second series). As the magnitude of the impulse potential increases, the texture becomes decisive [110] (Figure 8 c). At a constant potential exceeding -100... -150 V high-voltage pulse action does not lead to a qualitative change in texture [111] (Figure 9 a). Thus, there is a limiting nature of the energy of the constant potential at which there is an additional high-voltage pulse effect.

Calculations have shown that the characteristic energy of defect formation during ion implantation from plasma with the formation of a “thermal peak” is 500–700 eV for titanium nitride [8; 9]. Thus, at such energies, one can expect the appearance of “thermal peaks” in the case of isostructural zirconium

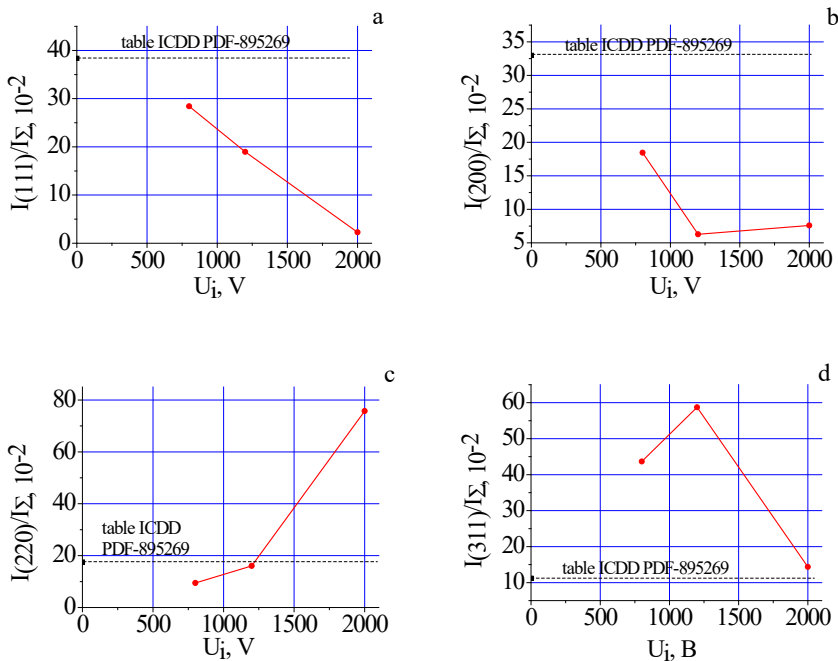


Figure 8. Dependence of the texture parameter P_{hkl} for the second series of ZrN coatings ($U_c = (0 \dots -27)$ V, $p_N = 0.63$ Pa) on the value of U_i for different planes: a – (111), b – (200), c – (220), d – (311)

nitride. As is known, in this case, as the collision energy increases, and with it the radius of the “thermal peak”, the time required to cool the collision zone to the initial temperature increases. Then, if the “thermal peak” lasts long enough, it gives the time required for significant atomic movements and relaxation, corresponding to local annealing. Thus, high-energy implantation, which generates “thermal peaks” with the time of its existence required to relax the stresses of the formed coatings, is an effective way to relieve internal stresses during deposition.

In this case, if the appearance of the predominant orientation [111] is determined by achieving a high level of compressive stresses, in particular, increasing the thickness of the coating of nitride coatings [10],

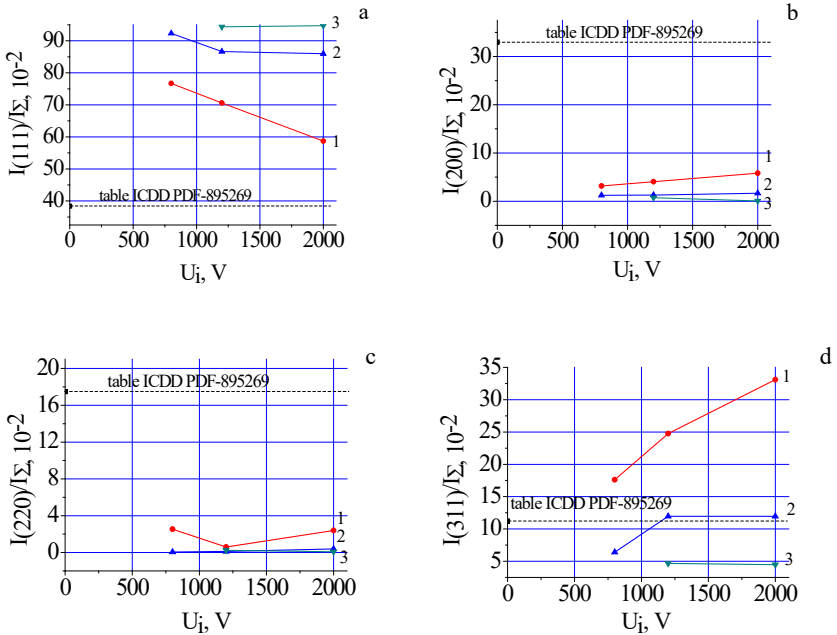


Figure 9. Dependence of the texture parameter P_{hkl} for the third series of ZrN coatings on the value of U_i for different planes: a – (111), b – (200), c – (220), d – (311); 1 – $U_c = -150$ V, $p_N = (0.133... 0.16)$ Pa; 2 – $U_c = -150$ V, $p_N = (0.4... 0.63)$ Pa, 3 – $U_c = -220$ V, $p_N = 0.63$ Pa

then removing the stress is the formation of texture [100], which has the lowest surface energy. Textures with an axis [110] or [311], which provides minimal radiation damage.

6. Substructural characteristics of ZrN coatings

The study of substructural characteristics was carried out by the method of approximating the shape of diffraction reflexes from two orders of reflection. The results are presented in table 1.

Analysis of substructural characteristics for ZrN coatings obtained by the first deposition scheme shows that at low pressures of 0.1 Pa and $U_c = -150$ V the size of the crystallites reaches 100 nm, and microdeformation

is the largest in this series 0.69 %. That is, at lower pressure and high $U_c = -150$ V, the energy loss on collision and the total energy loss is less due to the small number of atoms in the chamber volume, so this leads to such values of L and $\langle \varepsilon \rangle$. This may be due to the formation of the solid-soluble state Zr (N), lower zirconium nitride or cubic lattice zirconium nitride. This may be due to the process of polygonization with a sufficiently high mobility of film-forming particles deposited at low pressure. At the same time, the relatively low density of filling octahedral inter-nodes with nitrogen atoms allows to significantly relax the lattices arising during the deposition of microdeformation by the movement of dislocations and the formation of new boundaries.

Table 1

**Substructural characteristics of ZrN coatings
in different application schemes**

p_N, Pa	U_c, V	U_p, V	$\tau, \mu s$	L, nm	$\langle \varepsilon \rangle, \%$
The first deposition scheme					
0.133	-150	-	-	100	0.69
0.63	-30	-	-	10.2	0.25
0.63	-150	-	-	14.1	0.53
0.63	-220	-	-	300	0.65
The second deposition scheme					
063	-	-800	7	30.3	0.42
0.63	-27	-1200	7	40	0.36
0.63	-27	-2000	7	111	
The third deposition scheme					
0.16	-150	-800	7	142.8	0.57
0.133	-150	-1200	7	123.4	0.55
0.133	-150	-2000	7	200	0.56
0.4	-150	-800	7	300	0.74
0.63	-150	-1200	7	476.1	0.56
0.63	-150	-2000	7	163.9	0.48
0.63	-220	-1200	7	21.3	0.19
0.63	-220	-2000	7	21.7	0.22

At a nitrogen atmosphere pressure of 0.63 Pa and the lowest constant potential ($U_c = -30$ V), L and $\langle \epsilon \rangle$ have the lowest values of 10 nm and 0.25%, respectively. A further increase in U_c leads to the dependence of the microdeformation to an almost constant level (0.55 ... 0.6) % and to a significant increase in the average size of the crystallites in the direction of incidence of the film-forming particles. One of the main reasons for this process is the increase in the degree of interaction between nitrogen and metal atoms, activated by increasing energy. It should be noted that in this case there is the formation of crystallites of the columnar type (Figure 1 c) with the axis of the predominant orientation of growth [111] (Figure 2, spectra 3, 4). This change in substructural characteristics can be associated with the complete saturation of the formed coating with nitrogen atoms to stoichiometric and superstoichiometric nitrogen atoms. The latter determines the achievement of a constant value of lattice microdeformation and growth to larger values of crystallite sizes.

In ZrN coatings obtained by the second deposition scheme, microdeformation is less important, but there is an increase in the size of the crystallites (reaches a maximum of 100 nm) with increasing U_i . That is, there are processes of relaxation.

At the substructural level, the supply of high-voltage pulse potential under the simultaneous action of high constant potential (third scheme) in the formation of the coating leads to a decrease in microdeformation at low pressures (Table 1) and a smoother output values close to (0.5 ... 0.6) %. With increasing U_i in the entire pressure range, the deviation from the average value of microdeformation decreases. As mentioned above, the dependence on the almost constant value at high pressures is due to the filling of octahedral internodes with nitrogen atoms, which prevent deformation due to the strong bonds formed with metal atoms of the lattice. The supply of high-voltage pulses stimulates the activation of physico-chemical reactions, which leads to increased efficiency of the nitride formation process at relatively low pressures and thus the value of microdeformation remains at (0.5 ... 0.6)% in the entire pressure range (0.133 ... 0.63) Pa.

The supply of U_i leads to a qualitative change in the dependence of L on p_N . It is seen that in contrast to the pulseless mode, which is characterized by a decrease in the size of the crystallites at a pressure of 0.133 Pa, the supply of high-voltage pulses leads to an increase in the average size of

the crystallites. This dependence, which is observed during high-voltage pulse stimulation, can be explained by the higher energy transmitted by the deposited particles and, accordingly, their greater mobility and chemical activity in the formation of nitrides, which increases the perfection of the structure with increasing nitrogen pressure.

At the same time, the decrease in the size of crystallites at a high pressure of 0.63 Pa at the maximum amplitude of the pulse effect -2000 V is due to radiation exposure, which is associated with high energy particles deposited under pulsed high-voltage potential sufficient for cascading. In combination with the supersaturation of the coating by nitrogen atoms at high pressure, this leads to an increase in the number of nucleation sites and thus a decrease in the average crystallite size of the coating (Table 1).

Analyze the data in table 1. For the first technological scheme, the accumulation of defects is observed with increasing constant displacement potential and pressure of the nitrogen atmosphere. In the second technological mode there is a decrease in microdeformation as a result of relaxation, unfortunately the data is not enough, but given the typical dependence (affinity) with TiN, we can assume the same course of the graph with increasing pulse bias potential. The complex influence of constant and impulse displacement potentials first promotes the accumulation of defects, and when passing through the limit value $\cdot U_i = -1000 \text{ V} \dots -1500 \text{ V}$, relaxation processes are activated and as a result there is a decrease in crystallite size and microdeformation.

The integral parameter $PU = p_N (U_c + \tau \cdot f \cdot U_i)$ is proposed in the work for the analysis of the obtained data, and the voltage U was substituted modulo. It was found that for ZrN coatings with increasing values of the PU effect parameter, under the action of only a constant potential, the crystallite size (L) and microdeformation ($\langle \varepsilon \rangle$) increase as a result of increasing flux density, U_c and average temperature at the crystallization front. Under the action of U_i alone, relaxation processes within the nearsurface layers dominate with increasing PU due to greater thermal excitation in the pulse, which initiates the redistribution of defects, which in turn leads to a decrease in L and $\langle \varepsilon \rangle$. The simultaneous action of pulse and constant bias potentials is characterized by a similar accumulation of defects, as in the first case, and then by relaxation processes, which explains the decrease in the dependence

of L and $\langle \varepsilon \rangle$. Note that the maximum values of microhardness ≈ 43 GPa were obtained at $U_i = -850$ V and $U_c = -200$ V.

The above allows us to propose a model according to which a texture [110] with significant m macrostrains is formed in the near-surface zone as defects accumulate (vacancies, Frank loops, dislocations). But during the action of the impulse potential and the implantation of ions at a certain depth, the crystal lattice is rearranged to form a texture [100]. That is, there is not only a local restructuring of defects, but in such cases and due to the same restructuring the formation of a new texture. This leads to relaxation of both micro and macro stresses in its sublayer along with the texture [110] at other depths.

7. Macrostrained state of ZrN coatings

The results of the determination of macrostrain are presented in table 2. For coatings obtained according to the first deposition scheme, the formation of a uniaxial texture (axis [111]) is characteristic, especially in the range of constant potential values $-100 \dots -220$ V. For coatings of this type there is an increase in compression macrostrain with increasing U_c .

Table 2

Macrostrain of ZrN coatings for the first and third deposition schemes

The first deposition scheme		The third deposition scheme	
$p_N = 0.63$ Pa			
$U_i = 0$ V		$U_c = -220$ V	
U_c , V	ε , %	U_i , V	ε , %
150	-1.87	800	-
220	-2.15	1200	-2.06
-	-	2000	-2.23

For the third coating scheme, the supply of additional impulse potential leads to a reduction of macrostrain from -2.19 % to -1.78 % (Figure 10). The reason for this is the influence of relaxation processes due to the increase in temperature under the action of the impulse bias potential. Compression deformation is formed in all conditions of production.

In turn, the macrostrained state affects the functional properties of zirconium nitride coatings. Therefore, the effect of displacement potential on the hardness of coatings was further investigated.

8. Influence of bias potential on the hardness of ZrN coatings

The results of measuring hardness as the main express criterion of mechanical characteristics are presented in table. 3. At a lower pressure of 0.133 Pa, the hardness value reaches the level of 32-42 GPa. In the case of higher pressure of nitrogen atmosphere during deposition (0.63 Pa), the hardness remains almost constant at 37-38 GPa, this may be due to two mutually competing and opposite effects that affect hardness – saturation of the coating with nitrogen atoms, with the formation of strong covalent nitride bonds, and with a significant increase in the average size of crystallites (Table 1).

As for the influence of the constant potential on the hardness, its supply during deposition leads to a nonmonotonic effect of changes in microhardness (Table 3).

This change is the increase in hardness at the bias potential -100 V, which may be due to increased compression stress and greater efficiency of nitride formation. The decrease in hardness at a higher constant potential may be due to increased structural defects. However, in the range (-100 ... -150) V the hardness increases, translating the resulting coating into the category of superhard. As follows from the comparison with the substructural characteristics, the appearance of high hardness in this interval U_c with pulsed stimulation correlates with a decrease in the average size of crystallites (Table 1). Also, it is known that pulsed high-voltage stimulation increases the efficiency of nitride formation.

With increasing pressure there is an increase in the size of the crystallites while increasing the efficiency of nitride formation when applying U_i act as opposing factors influencing the mechanical properties of coatings, which is manifested in a small change in hardness (Table 3).

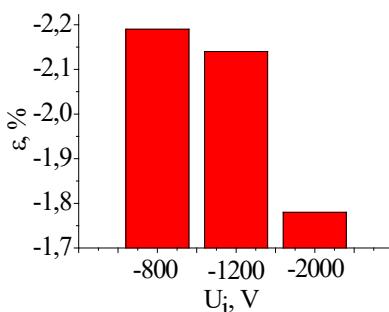


Figure 10. Histogram of the dependence of macrostrain on the value of the impulse potential for ZrN coatings obtained at $U_c = -150$ V, $p_N = 0.63$ Pa, $\tau = 7 \mu s$

Dependence of hardness of ZrN coatings on deposition conditions

Deposition conditions						
	Without impulse influence ($U_i = 0$ V)			Additional pulse stimulation ($U_c = -150$ V, $\tau = 7$ μ s)		
	U_c , V			U_i , V		
	30	150	220	800	1200	2000
p_N , Pa	H, GPa					
0.133	-	-	-	39.5	42.5	32
0.63	38	41	36	39	33	40

Leaving the maximum value of hardness at a high level (40-43) GPa increase of particle energy during coating formation by feeding U_i leads to shift of the position of the maximum on the pressure scale: with increasing U_i the maximum hardness shifts to the region of higher working pressures of nitrogen atmosphere during coating formation. The factor that leads to a decrease in hardness at high pressures can be considered an increase in the average size of crystallites, which is associated with pulsed high-energy effects (Table 1). However, it can be noted that the use of pulsed mode avoids catastrophically large grain growth, which can impair mechanical properties, and which could be expected in the case of high-energy exposure to particles accelerated by applying a continuous high-voltage bias potential.

Due to the decrease in the average energy of the accelerated particles at high pressure, there is a decrease in the size of the crystallites, and this is the main factor that causes some increase in hardness found for this type of coating.

With respect to ZrN coatings, at high values of U_c (-200 V), in the whole range of pulse potentials, the formation of the texture with the axis [111], in contrast to TiN coatings, in which under such deposition conditions formed radiation-stimulated texture [110].

9. Conclusions

The scientific problem was solved in the work, which was to obtain nanostructured and high-strength vacuum-arc nitride coatings ZrN, as well as to establish the physical essence of the influence of deposition parameters on the structure of these coatings. It is established that:

1. Under the action of only a constant bias potential, the texture changes. With increasing U_c from -27 V to -220 V there is a transition from [100] to the bitexture state [111] + [311] and subsequently to [111]. At the substructural level (first scheme) with increasing U_c , the values of both crystallite size (L) and micro-deformation ($\langle \varepsilon \rangle$) increase, and at the same time ZrN coatings have high values of macrodeformation level ($\varepsilon = -1.87\% \dots -2.15\%$) and due to this, these coatings have a high hardness ($H = 41$ GPa). It should be noted that this maximum is observed at $U_c = -150$ V.

2. The supply of the impulse bias potential ($U_i = -800$ V) stimulates the formation of the bitexture state with texture axes [111] + [311], even at the lowest $U_c = -27$ V further increase in U_i causes the appearance of radiation-stimulated texture [110]. The size of the crystallites and microdeformation increase with increasing U_i , this is due to the additional impulse effect, which at low values of U_c leads to the enlargement of the crystalline grains. Hardness remains almost constant at 37-38 GPa.

3. The pressure of the nitrogen atmosphere in the process of deposition of ZrN coatings has a great contribution to the peculiarities of structure formation. Thus, at the lowest pressure ($p_N = 0.133$ Pa) with the simultaneous action of $U_c = -150$ V and the growth of U_i is the formation of the bitexture state [111] + [311], with virtually no texture [110]. At the same time, L and $\langle \varepsilon \rangle$ increase due to the high level of macro stresses ($\varepsilon = -2.0\% \dots -2.2\%$), these coatings have a high hardness at the level of 40... 42 GPa in the pulse potential range -1000... -1200 V.

4. In the case of $U_c = -220$ V, $p_N = 0.63$ Pa and increase of U_i , a texture is formed [111], almost as for ZrN coatings obtained by the first deposition scheme.

5. It is shown that the hardness of nitride coatings is determined by the type of axial texture, substructure parameters, and macrostrain. The influence parameter $p_N \cdot (U_c + \tau \cdot f \cdot U_i)$ is proposed, which allows to establish intervals corresponding to a high level of hardness on the dependences of microdeformation values and crystal size.

References:

1. Vasylyev M. A., Mordyuk B. N., Sidorenko S. I., Voloshko S. M., Burmak A. P., Kruhlov I. O., Zakiev V. I. (2019) Characterization of ZrN coating low-temperature deposited on the preliminary Ar⁺ ions treated 2024 Al-alloy. *Surf. Coat. Technol.*, vol. 361, pp. 413–424.

2. Mareus R., Mastail C., Angay F., Brunetière N., Abadias G. (2020) Study of columnar growth, texture development and wettability of reactively sputter-deposited TiN, ZrN and HfN thin films at glancing angle incidence. *Surf. Coat. Technol.*, vol. 399, pp. 126130.
3. Zhu F., Zhu K., Hu Y., Ling Y., Wang D., Peng H., Xie Z., Yang R., Zhang Z. (2019) Microstructure and Young's modulus of ZrN thin film prepared by dual ion beam sputtering deposition. *Surf. Coat. Technol.*, vol. 374, pp. 997–1005.
4. Horoshih V. M., Leonov S. A., Belous V. A., Vasilenko R. L., Kolodij I. V., Kuprin A. S., Tihonovskij M. A., Tolmacheva G. N. (2014) Struktura i mehani-cheskie svoystva pokrytij ZrN, poluchaemyh osazhdeniem potokov plazmy vakuumnoj dugi [Structure and mechanical properties of ZrN coatings obtained by deposition of vacuum arc plasma flows]. *Physical surface engineering*, vol. 12, no. 1, pp. 45–56. (in Russian)
5. Umansky Ya. S., Skakov Yu. A., Ivanov A. N. etc. (1982) Kristallografija, rentgenografija i jelektronnaja mikroskopija [Crystallography, radiography and electron microscopy]. Moscow: Metallurgiya, 632 p. (in Russian)
6. Palatnik L. S. (1983) Struktura i fizicheskie svoystva tverdogo tela. Laboratornyj praktikum [Structure and physical properties of a solid body. Laboratory workshop]. Kyiv: Higher School, 264 p. (in Russian)
7. Mirkin L. I. (1976) Rentgenostrukturnyj analiz. Poluchenie i izmerenie rentgenogramm: Spravochnoe rukovodstvo [X-ray diffraction analysis. Obtaining and measuring radiographs: A reference guide]. Moscow: Science, 326 p. (in Russian)
8. Bilek M. M. M., McKenzie D. R., Rarrant R., Lim S., McCulloch D. G. (2002) Plasma-based ion implantation utilising a cathodic arc plasma. *Surf. Coat. Technol.*, vol. 156, no. 1–3, pp. 136–142.
9. Sobol' O. V., Andreev A. A., Grigoriev S. N., Gorban' V. F., Volosova M. A., Aleshin S. V., Stolbovoi V. A. (2012) Effect of high-voltage pulses on the structure and properties of titanium nitride vacuum-arc coatings. *Metal Science and Heat Treatment*, vol. 54, no. 3–4, pp. 195–203.
10. Lima S. H. N., McCulloch D. G., Bilek M. M. M., McKenzie D. R. (2003) Minimisation of intrinsic stress in titanium nitride using a cathodic arc with plasma immersion ion implantation. *Surface and Coatings Technology*, vol. 174–175, pp. 76–80.